

## **Influence of OH<sup>-</sup> concentration on the illitization of kaolinite at high pressure**

M. Mantovani (a), A. Escudero (b), A.I. Becerro (a)

(a) Instituto de Ciencia de Materiales de Sevilla, Dpto. Química Inorgánica (CSIC-US), c/ Américo Vespucio, 49, 41092 Sevilla, Spain

(b) Bayerisches Geoinstitut, Universität Bayreuth, D-95440 Bayreuth, Germany

### **Abstract**

The products of hydrothermal reactions of kaolinite at 300 °C and 1000 bars were studied in KOH solutions covering an OH<sup>-</sup> concentration, [OH<sup>-</sup>], of 1 M to 3.5 M. XRD patterns indicated a notable influence of the [OH<sup>-</sup>] on the reaction. At [OH<sup>-</sup>] ≥ 3 M, the only stable phase was muscovite/illite. The content of muscovite/illite was calculated from the analysis of the diagnostic 060 reflections of kaolinite and muscovite/illite. The results showed a linear dependence of kaolinite and muscovite/illite contents with [OH<sup>-</sup>]. <sup>27</sup>Al MAS NMR spectroscopy revealed the formation of small nuclei of K-F zeolite at high [OH<sup>-</sup>]. Finally, modelling of the <sup>29</sup>Si MAS NMR spectra indicated that the Si/Al ratio of the muscovite/illite formed was very close to that of muscovite, at least in the mineral formed at low [OH<sup>-</sup>]. In good agreement with the XRD data, the quantification of the reaction products by <sup>29</sup>Si MAS NMR indicated a linear decrease of the kaolinite content with increasing OH<sup>-</sup> concentration.

### **Keywords**

Kaolinite; KOH; Muscovite/illite; Hydrothermal reaction; OH<sup>-</sup> concentration; XRD; NMR

### **1. Introduction**

The presence of alkaline fluids in kaolinite-rich sediments during burial-tectonic diagenesis as subduction zones caused dissolution of kaolinite and precipitation of illite and other potassium phases (Kisch, 1983). Since Velde (1965) synthesized muscovite from kaolinite and KOH solutions, results on the illitization of kaolinite at different temperatures and pH values were reported by several authors. Huang (1993) studied the conversion of kaolinite into illite in 2.58 M KOH solution at 225–350 °C. Comparison of his results with those of kaolinite illitization in a near-neutral KCl solution (Chermak and Rimstidt, 1990) revealed that the conversion was two to three orders of magnitude faster at alkaline than at neutral conditions. Huang (1993) observed that the unusually high conversion rate in the highly alkaline solution was not predicted from the kinetics model derived from near-neutral KCl solutions. He suggested a systematic experimental program with a wide pH range to quantify the pH effect on the illitization rates. Bauer and Berger (1998) studied the dissolution rate of kaolinite at 35 °C and 80 °C in KOH solutions and found an increase in the activation energy from 33 ± 8 kJ/mol in a 0.1 M KOH solution to 51 ± 8 kJ/mol in a 3 M KOH solution. Bauer et al. (1998) reported, under the same conditions, that KOH concentration influenced the type of precipitation products, and kaolinite and illite were the only products obtained at low OH<sup>-</sup> concentrations.

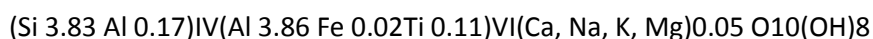
Precipitation of KI-zeolite and K-feldspar was observed at higher OH concentrations. More recently, Bentabol et al. (2003) investigated the illitization of kaolinite in the presence of aqueous solutions containing variable amounts of KOH, NaOH and of MgCl<sub>2</sub> at 200 °C and 300 °C. The initial pH of the solutions ranged from 12.3 to 13.6. At 200 °C recrystallization of kaolinite was accompanied by formation of illite, and analcime was observed as a transitional phase. The trend was similar at 300 °C, though mica formation was observed after shorter reaction times and mica composition showed deviation from dioctahedral form to trioctahedral phlogopite due to the presence of Mg in the system. Although different reaction products were obtained in each reaction, they could not be explained on the basis of different pH values, because the reactions differed, as well, in the nature of the cations added to the system (K, Na and Mg).

The present study was designed to investigate the influence of [OH<sup>-</sup>] in the illitization of kaolinite in the absence of other cations than K<sup>+</sup>. The [OH<sup>-</sup>] range studied is from 1 M to 3.5 M. X-ray powder diffraction was used to identify and quantify new crystalline phases while <sup>29</sup>Si and <sup>27</sup>Al MAS NMR (Magic Angle Spinning Nuclear Magnetic Resonance) spectroscopy was used to observe any Si- and Al-containing phases not detected by diffraction, as well as to quantify the percentage of Si-containing phases.

## 2. Materials and methods

### 2.1. Kaolinite

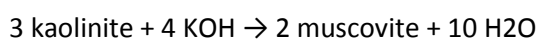
All the experiments reported in the present study were performed on KGa-1b kaolinite with chemical formula:



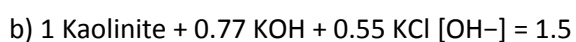
and molar mass 518.7. The mineral was supplied by the Source Clay Minerals Repository of The Clay Minerals Society ([www.clays.org](http://www.clays.org)).

### 2.2. Hydrothermal reactions

KOH solutions were prepared to cover a [OH<sup>-</sup>] range from 1 to 3.5 M. All solutions contained a minimum supply of K<sup>+</sup> as to allow complete transformation of kaolinite in muscovite/illite1 assuming the reaction:



(calculated on the basis of the unit formula of kaolinite containing 4 tetrahedral sites, as given above for KGa-1b). This assumption is reasonable since the composition of the illite formed was close to muscovite. Extra K<sup>+</sup> necessary for this stoichiometry was added in the form of KCl. Kaolinite (100 mg) was dispersed in 100 μL of aqueous solutions containing KOH and KCl in the following molar proportions:



c) 1 Kaolinite + 1.03 KOH + 0.29 KCl [OH<sup>-</sup>] = 2.0

d) 1 Kaolinite + 1.29 KOH + 0.03 KCl [OH<sup>-</sup>] = 2.5

e) 1 Kaolinite + 1.53 KOH [OH<sup>-</sup>] = 3.0

f) 1 Kaolinite + 1.81 KOH [OH<sup>-</sup>] = 3.5

The experiments were performed in gold tubes of 30-mm length, 5 mm o.d. and 4 mm i.d. The tubes were welded shut, weighed, flattened to eliminate free space within the experimental volume and placed in stainless-steel hydrothermal reactors in horizontal resistance furnaces (High Pressure Hydrothermal Laboratory, Bayerisches Geoinstitut Bayreuth, Germany). An external pressure of 1000 bars was applied, and the temperature was controlled via internal thermocouples and was maintained constant at 300 °C (± 2 °C) for 24 h. Temperature and pressure of hydrothermal reactions were selected as to obtain illitization of kaolinite within a reasonable period of time (Mantovani, in press and Mantovani et al., 2010). At the end of the runs the reactors were quickly cooled down to room temperature with compressed air, and each capsule was weighed, cut and open. The slightly moistened powder obtained was washed with distilled water, filtered and dried at room temperature. Separation of the liquid and solid phases was not possible due to the high solid/liquid ratio employed. For this reason, the present study did not report on the liquid product composition like other related studies did.

### 2.3. Characterization techniques

X-ray powder diffraction (XRD) patterns were recorded using a PANalytical X'Pert Pro diffractometer with Ni-filtered CuK $\alpha$  radiation, steps of 0.02 °2 $\theta$ , and counting time of 160 s. To measure quantitatively the relative amounts of kaolinite and muscovite/illite in the reaction products, additional XRD patterns were taken in the 58–64 °2 $\theta$  range with steps of 0.03 °2 $\theta$  and a counting time of 500 s. The selected region of each pattern was fitted using the ProFit 1.0c software (Philips Analytical X-ray (1996) Philips Electronics N.V.) to two PseudoVoigt functions (corresponding to the 060 reflections of muscovite/illite and kaolinite). An XRD calibration curve prepared from a series of mixtures containing various proportions of kaolinite and muscovite/illite showed a linear relationship between the 060 areas ratio and the relative quantities of muscovite/illite and kaolinite (Mantovani and Becerro, in press). The areas under the curve of the 060 reflections of kaolinite and muscovite/illite provided, therefore, a direct measurement of the relative quantities of both minerals in a sample containing them as dominant products. The relative uncertainty of measuring muscovite/illite content in the products was considered to be ± 5%. Magic Angle Spinning Nuclear Magnetic Resonance (MAS NMR) spectra were recorded in a Bruker DRX400 (9.39 T) spectrometer equipped with a multinuclear probe, using 4 mm zirconium rotors spinning at 10 kHz. <sup>29</sup>Si MAS NMR single pulse experiments were carried out with a pulse length of 2.5  $\mu$ s ( $\pi/2$  pulse length = 7.5  $\mu$ s), an observation frequency of 79.49 MHz, and an optimized delay time of 40 s. The chemical shifts were reported in ppm related to tetramethylsilane. A modified version of the Bruker Winfit program, which handles the finite spinning speed in MAS experiments (Massiot et al., 2002), was used for the modelling of the <sup>29</sup>Si MAS NMR spectra. Single pulse <sup>27</sup>Al MAS NMR spectra were recorded at 104.26 MHz with a pulse length of 1.1  $\mu$ s ( $\pi/2$  pulse length = 11  $\mu$ s) and a delay time of 0.5 s. The chemical shifts were reported in ppm related to a 0.1 M AlCl<sub>3</sub> solution.

### 3. Results and discussion

#### 3.1. XRD results

Representative sections of the X-ray diffraction diagrams of kaolinite KGa-1b before and after the hydrothermal reactions are shown in Fig. 1. The diagram of the sample reacted with a  $[\text{OH}^-] = 1 \text{ M}$  (reaction a) showed the unchanged typical reflections of the starting material and a series of new reflections that indicated crystallization of muscovite/illite (1 M polytype, ICDD-PDF cards 29-1496 and 07-0025). The location of the 060 reflection of kaolinite corresponded to a  $d_{060}$  value of  $1.503 \text{ \AA}$ , larger than that of the parent kaolinite ( $1.490 \text{ \AA}$ ). The XRD patterns of the products of reactions (b), (c) and (d) showed an increase in the intensity of muscovite/illite reflections, while the kaolinite reflections tend to disappear with increasing  $[\text{OH}^-]$ . No reflections corresponding to any additional new phases were observed in the patterns. Finally, extreme  $[\text{OH}^-]$  values had a very aggressive effect on the kaolinite structure. The kaolinite reflections disappeared in the XRD patterns of reactions e and f (corresponding to  $[\text{OH}^-] = 3 \text{ M}$  and  $3.5 \text{ M}$ , respectively), whereas muscovite/illite appeared as the only stable phase. The anatase reflection, present in the pattern of unreacted kaolinite could be observed more clearly in the pattern of the product obtained at the most extreme conditions due to the disappearance of the kaolinite 002 reflection (at  $24.9^\circ 2\theta$ ).

Two diagnostic reflections were chosen to measure quantitatively the relative amounts of kaolinite and muscovite/illite in the reaction products: The 060 reflection of kaolinite at  $62.33^\circ 2\theta$  and the 060 reflection of muscovite/illite at  $61.73^\circ 2\theta$ . The muscovite/illite reflection increased as the kaolinite reflection decreased with increasing  $\text{OH}^-$  concentration (Fig. 2). The mass content of muscovite/illite increased linearly with increasing  $\text{OH}^-$  concentration while the mass of kaolinite decreased (Fig. 3). A complete conversion of kaolinite into muscovite/illite was reached after 24 h of hydrothermal reaction at 1000 bars and  $300^\circ \text{C}$  in the  $3.5 \text{ M}$  KOH solution.

#### 3.2. $^{27}\text{Al}$ MAS NMR spectroscopy

The  $^{27}\text{Al}$  MAS NMR spectra of the reaction products of kaolinite reacted for 24 h at  $300^\circ \text{C}$  and increasing  $\text{OH}^-$  concentration are shown in Fig. 4. The spectrum of the starting kaolinite consisted of a signal centred at  $1.5 \text{ ppm}$  corresponding to the aluminum ions in the octahedral sheet (Müller et al., 1981). This  $\text{VIAl}$  signal shifted towards higher frequencies with increasing  $[\text{OH}^-]$  of the KOH solutions in agreement with the fact that  $\text{VIAl}$  in pure muscovite/illite was expected at  $\sim 3.4 \text{ ppm}$  (Mantovani et al., 2010). In addition, this signal became asymmetric as a result of a quadrupolar interaction of the  $\text{VIAl}$  site of the muscovite/illite phase. When kaolinite was reacted at  $300^\circ \text{C}$  for 24 h in the  $[\text{OH}^-] = 1.0 \text{ M}$  solution, a new band with maximum at  $\sim 69 \text{ ppm}$  was observed which can be assigned to  $\text{IVAl}$  nuclei in the muscovite/illite phase (Sanz and Serratosa, 1984), in agreement with the XRD pattern. A second signal at  $61 \text{ ppm}$  developed with increasing  $[\text{OH}^-]$  concentration. Mantovani et al. (2010) demonstrated that this latter signal must be assigned to  $\text{IVAl}$  nuclei in K-F zeolite domains whose coherent diffraction sizes were not big enough as to be detected by X-ray diffraction. Previous studies showed that this signal decreased with increasing time at a given pressure (Mantovani et al., 2009) and with increasing pressure at a given time (Mantovani et al., 2010). However, these studies showed that the amount of K-F zeolite increased with

increasing  $[\text{OH}^-]$  concentration. This fact is in agreement with the higher stability of K-F zeolite in higher alkaline media (Barth-Wirsching et al., 1993). The fact that  $^{27}\text{Al}$  is a quadrupolar nucleus hinders any quantitative analysis of the phases.

### 3.3. $^{29}\text{Si}$ MAS NMR spectroscopy

The  $^{29}\text{Si}$  MAS NMR spectra of kaolinite before and after the hydrothermal reaction at  $300\text{ }^\circ\text{C}$  for 24 h in solutions of increasing  $[\text{OH}^-]$  are shown in Fig. 5. Kaolinite displayed a single symmetric signal at  $-91.5\text{ ppm}$ , corresponding to  $\text{Q3(0Al)}$  units in the tetrahedral sheet of kaolinite (Kinsey et al., 1985). The hydrothermal reaction in the 1 M KOH solution yielded a broad band on the high frequency side of the kaolinite resonance. The band was compatible with the Si resonances in muscovite/illite, expected at  $-89.5\text{ ppm}$ ,  $-86.5\text{ ppm}$  and  $-83.0\text{ ppm}$  for  $\text{Q3(0Al)}$ ,  $\text{Q3(1Al)}$  and  $\text{Q3(2Al)}$ , respectively (Weiss et al., 1987). The intensity of the band increased with increasing  $[\text{OH}^-]$  while the kaolinite resonance decreased. These observations were in agreement with the XRD data.

To obtain structural information about the muscovite/illite phase and to quantify the content of kaolinite and muscovite/illite in the reaction products, the  $^{29}\text{Si}$  MAS NMR spectra were decomposed into their individual components (Table 1). In the case of the samples reacted in lower  $[\text{OH}^-]$  solutions, the spectra were fitted by 4 Lorentzian lines accounting for the Si environments expected in kaolinite and muscovite/illite. The spectra of the samples at  $[\text{OH}^-] = 2.5, 3.0$  and  $3.5\text{ M}$  were fitted by two additional lines at  $\sim -101$  and  $-96\text{ ppm}$  which were assigned to  $\text{Q4(mAl)}$  ( $m = 1$  and  $2$ ) units in a tectoaluminosilicate phase (Lippmaa et al., 1980), not detected in the X-ray diffraction patterns. The corresponding  $^{27}\text{Al}$  NMR signals were expected at  $54\text{--}69\text{ ppm}$ , which is typical of Al in tetrahedral coordination with four next-nearest silicon neighbours. They could not be observed due to overlapping with high intensity signals of Al in K-F zeolite and muscovite/illite. The zeolite phase detected in the  $^{27}\text{Al}$  MAS NMR spectra of samples reacted in solutions of higher KOH concentration was expected to produce a  $^{29}\text{Si}$  resonance at  $\sim -85.6\text{ ppm}$  (Engelhardt and Michel, 1987). Attempts to separate this signal from the  $\text{Q3(1Al)}$  muscovite/illite resonance were unsuccessful because of their proximity. The intensity of the signal at  $\sim -86\text{ ppm}$  in the samples reacted in solutions of  $[\text{OH}^-] \geq 2\text{ M}$  was, therefore, due to the  $\text{Q3(1Al)}$  environment in muscovite/illite and Si in K-F zeolite.

Si/Al ratios in the tetrahedral sheet of muscovite/illite were calculated assuming the absence of  $\text{AlOAl}$  linkages (Loewenstein's rule, Engelhardt and Michel, 1987). The Si/Al ratio decreased with increasing  $[\text{OH}^-]$  (Table 1). However, the data of the samples reacted in solutions with  $[\text{OH}^-] \geq 2.0\text{ M}$  were affected by the K-F zeolite signal. Fittings of the  $^{29}\text{Si}$  NMR spectra of samples reacted in  $[\text{OH}^-] = 1.0\text{ M}$  and  $1.5\text{ M}$  (that did not show any appreciable Al signal from K-F zeolite) indicated that the Si/Al ratio in the muscovite/illite phase formed was close to 3. This value indicated that the composition of the illite formed was close to muscovite. Huang (1993) synthesized muscovite/illite from kaolinite at 500 bars from  $2.58\text{ M}$  KOH solutions. His EDX results indicated that the illite formed has a composition close to muscovite, in agreement with our  $^{29}\text{Si}$  NMR results.

Finally, the area under the curve corresponding to the  $^{29}\text{Si}$  NMR resonance of kaolinite was plotted versus  $[\text{OH}^-]$  of the solution (Fig. 6). The kaolinite content in the reaction product decreased linearly with increasing  $\text{OH}^-$  concentration, in good agreement with the XRD data.

However, in contrast with the XRD data, a low content of Si in kaolinite was still observed at very high OH concentrations. These Si nuclei were likely forming part of very small crystallites of kaolinite, not detected by XRD.

#### **4. Conclusions**

Kaolinite illitization was investigated at constant pressure, temperature and time in KOH solutions. XRD data showed a linear dependence of kaolinite and muscovite/illite contents with  $[\text{OH}^-]$ . While the XRD data showed a direct transformation of kaolinite into muscovite/illite, the  $^{27}\text{Al}$  MAS NMR spectra revealed the formation of small nuclei of K-F zeolite when high  $[\text{OH}^-]$  solutions were used in the hydrothermal reactions.  $^{29}\text{Si}$  MAS NMR data also showed a linear decrease of the kaolinite content with increasing  $[\text{OH}^-]$ . However, in contrast with XRD results, the NMR data indicated that some Si nuclei forming part of kaolinite were still present in the samples reacted in very high  $[\text{OH}^-]$  solutions. Fitting of the  $^{29}\text{Si}$  MAS NMR spectra of the reaction products indicated that the illite formed had a composition very close to muscovite

#### **Acknowledgements**

Bayerisches Geoinstitut is acknowledged for use of its Hydrothermal Lab. Supported by European Union VI Framework Programme as an HRM Activity (Contract number MRTN-CT-2006-035957), DGICYT (Project no. CTQ2007-63297) and Junta de Andalucía (Excellence Project P06-FQM-02179).

## References

A. Bauer, G. Berger

Kaolinite and smectite dissolution rate in high molar KOH solutions at 35 °C and 80 °C

Applied Geochemistry, 13 (1998), pp. 905–916

A. Bauer, B. Velde, G. Berger

Kaolinite transformation in high molar KOH solutions

Applied Geochemistry, 13 (1998), pp. 619–629

S.W. Bailey, S.W. Bailey

Classification and structures of micas ,in: S.W. Bailey (Ed.), Micas, Reviews in Mineralogy, vol 13 Mineralogical Society of America, Washington, D.C (1984), pp. 1–12

U. Barth-Wirsching, H. Höller, D. Klammer, B. Konrad

Synthetic zeolites formed from expanded perlite: type, formation conditions and properties

Mineralogy and Petrology, 48 (1993), pp. 275–294

M. Bentabol, M.D. Ruiz Cruz, F.J. Huertas, J. Linares

Hydrothermal transformation of kaolinite to illite at 200 and 300 °C

Clay Minerals, 38 (2003), pp. 161–172

J.A. Chermak, J.D. Rimstidt

The hydrothermal transformation rate of kaolinite to muscovite/illite

Geochimica et Cosmochimica Acta, 54 (1990), pp. 2979–2990

G. Engelhardt, D. Michel

High Resolution Solid State NMR of Silicates and Zeolites

John Wiley and Sons, New York (1987)

W.L. Huang

The formation of illitic clays from kaolinite in KOH solution from 225 °C to 350 °C

Clays and Clay Minerals, 41 (1993), pp. 645–654

R.A. Kinsey, R.J. Kirkpatrick, J. Hower, K.A. Smith, E. Oldfield

High-resolution <sup>27</sup>Al and <sup>29</sup>Si Nuclear Magnetic-Resonance spectroscopic study of layer silicates, including clay-minerals

American Mineralogist, 70 (1985), pp. 537–548

H.J. Kisch

Mineralogy and petrology of burial diagenesis (burial metamorphism) and incipient metamorphism in clastic rocks, in: G. Larsen, G.V. Chilinger (Eds.), Diagenesis in Sediments and Sedimentary Rocks, Vol. 2 Elsevier, Amsterdam (1983), pp. 289–493

E. Lippmaa, M. Magi, A. Samoson, G. Engelhardt, A.R. Grimmer

Structural studies of silicates by solid-state high-resolution Si-29 NMR

Journal of the American Chemical Society, 102 (1980), pp. 4889–4893

M. Mantovani, A. Escudero, A.I. Becerro

Application of <sup>29</sup>Si and <sup>27</sup>Al MAS NMR spectroscopy to the study of the reaction mechanism of kaolinite to illite/muscovite

Clays and Clay Minerals, 57 (2009), pp. 302–310

M. Mantovani, A. Escudero, A.I. Becerro

Effect of pressure on kaolinite illitization

Applied Clay Science, 50 (2010), pp. 342–347

Mantovani, in press



Mantovani, M., Becerro, A.I., in press. Illitization of kaolinite: The effect of pressure on the reaction rate. *Clays and Clay Minerals*.

D. Massiot, F. Fayon, M. Capron, I. King, S. Le Calvé, B. Alonso, J.O. Durand, B. Bujoli, Z. Gan, G. Hoatson

Modelling one- and two-dimensional solid state NMR spectra

*Magnetic Resonance in Chemistry*, 40 (2002), pp. 70–76

D. Müller, W. Gessner, H.J. Behrens, G. Scheller

Determination of the aluminum coordination in aluminum-oxygen compounds by solid-state high-resolution Al-27 NMR

*Chemical Physics Letters*, 79 (1981), pp. 59–62

J. Sanz, J.M. Serratosa

Si-29 and Al-27 high resolution MAS-NMR spectra of phyllosilicates

*Journal of the American Chemical Society*, 106 (1984), pp. 4790–4793

B. Velde

Experimental determination of muscovite polymorph stabilities: *American mineralogist*, 50 (1965), pp. 436–449

C.A. Weiss, S.P. Altaner, R.J. Kirkpatrick

High-resolution <sup>29</sup>Si NMR spectroscopy of 2:1 layer silicates: correlations among chemical shift, structural distortions, and chemical variations

*American Mineralogist*, 72 (1987), pp. 935–942

## Figure captions

**Figure 1.** XRD patterns of kaolinite before (top) and after hydrothermal reaction at 300 °C for 24 h in aqueous solutions of increasing [OH<sup>-</sup>]. a: [OH<sup>-</sup>] 1.0 M, b: [OH<sup>-</sup>] 1.5 M, c: [OH<sup>-</sup>] 2.0 M, d: [OH<sup>-</sup>] 2.5 M, e: [OH<sup>-</sup>] 3.0 M, and f: [OH<sup>-</sup>] 3.5 M. \*: Reflections from muscovite/illite. Ant: anatase reflections.

**Figure 2.** Selected portions of the XRD patterns of kaolinite reacted at 300 °C for 24 h in aqueous solutions of increasing [OH<sup>-</sup>]. a: [OH<sup>-</sup>] 1.0 M, b: [OH<sup>-</sup>] 1.5 M, c: [OH<sup>-</sup>] 2.0 M, d: [OH<sup>-</sup>] 2.5 M, and f: [OH<sup>-</sup>] 3.5 M. The patterns show the 060 reflections of kaolinite and muscovite/illite. Dotted line (experimental); solid lines (calculated).

**Figure 3.** Content of kaolinite and muscovite/illite with increasing OH<sup>-</sup> concentrations derived from the XRD data.

**Figure 4.** <sup>27</sup>Al MAS NMR spectra of kaolinite before and after hydrothermal reaction at 300 °C for 24 h in aqueous solutions of increasing [OH<sup>-</sup>]. a: [OH<sup>-</sup>] 1.0 M, b: [OH<sup>-</sup>] 1.5 M, c: [OH<sup>-</sup>] 2.0 M, d: [OH<sup>-</sup>] 2.5 M, e: [OH<sup>-</sup>] 3.0 M, and f: [OH<sup>-</sup>] 3.5 M. SSB=Spinning Side Band.

**Figure 5.** <sup>29</sup>Si MAS NMR spectra of kaolinite before and after hydrothermal reaction at 300 °C for 24 h in aqueous solutions of increasing [OH<sup>-</sup>]. a: [OH<sup>-</sup>] 1.0 M, b: [OH<sup>-</sup>] 1.5 M, c: [OH<sup>-</sup>] 2.0 M, d: [OH<sup>-</sup>] 2.5 M, e: [OH<sup>-</sup>] 3.0 M, and f: [OH<sup>-</sup>] 3.5 M.

**Figure 6.** Si content in kaolinite versus [OH<sup>-</sup>] of the solutions, derived from the <sup>29</sup>Si MAS NMR data.

**Table 1**

Table 1. Chemical shift values in ppm and area under the curve (in parenthesis) obtained after fitting the experimental  $^{29}\text{Si}$  MAS NMR spectra to the different Si environments present in the samples.

Type of Si environment	1.0 M	1.5 M	2.0 M	2.5 M	3.0 M	3.5 M
Kaolinite Q <sup>3</sup> (0Al)	-91.2 (63)	-91.3 (54)	-91.2 (30)	-91.4 (24)	-91.7 (11)	-91.9 (9)
M/I Q <sup>3</sup> (0Al)	-88.1 (10)	-88.1 (10)	-89.3 (9)	-88.4 (11)	-89.2 (10)	-89.8 (8)
M/I Q <sup>3</sup> (1Al) + K-F zeolite	-85.9 (15)	-86.0 (21)	-86.1 (35)	-85.9 (32)	-86.3 (39)	-86.3 (39)
M/I Q <sup>3</sup> (2Al)	-82.5 (12)	-82.6 (15)	-82.6 (26)	-82.3 (22)	-82.9 (27)	-82.9 (37)
Amorphous Q <sup>3</sup> (mAl)				-101.8 (5)	-101.3 (7)	-101.0 (4)
Amorphous Q <sup>3</sup> (mAl)	-	-	-	-96.5 (6)	-95.2 (6)	-96.8 (3)
Si/Al ratio in M/I	2.8	2.7	-	-	-	-

Figure 1

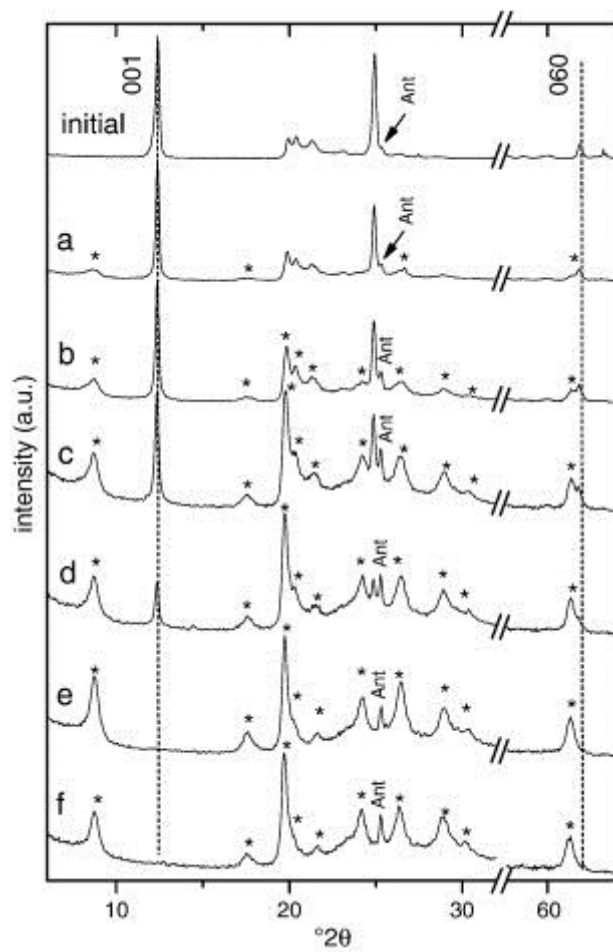


Figure 2

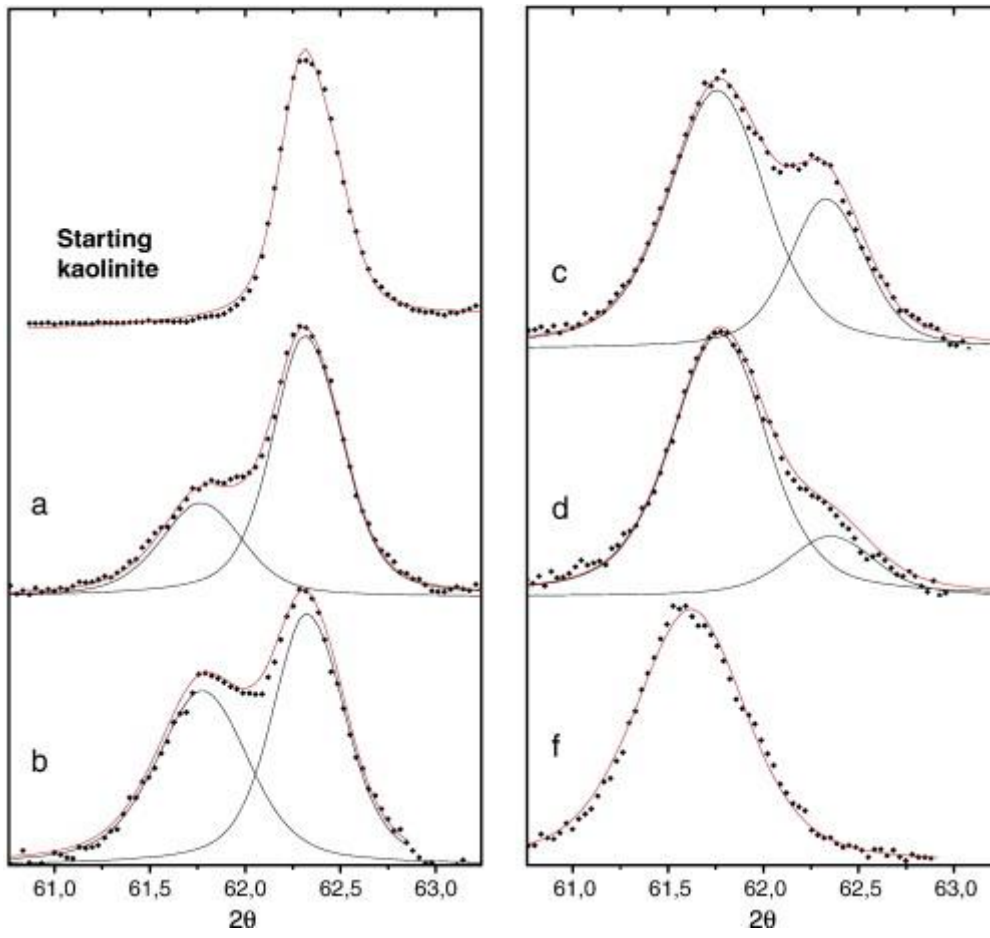


Figure 3

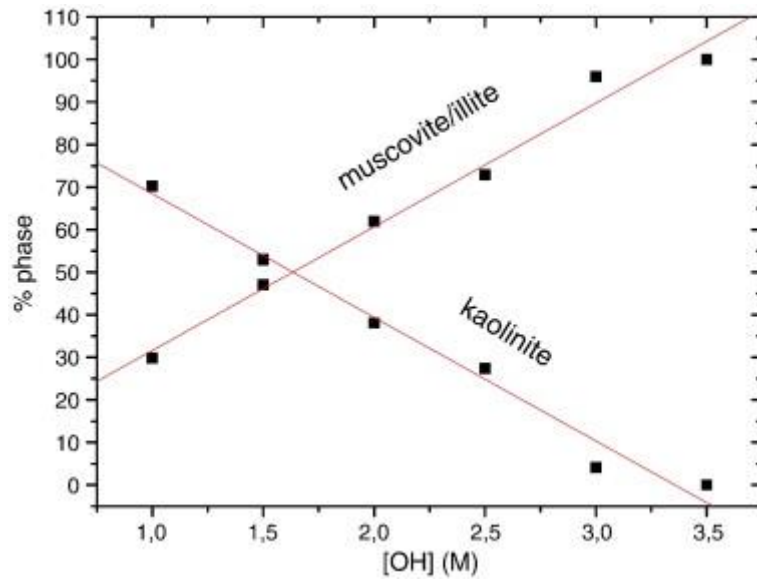


Figure 4

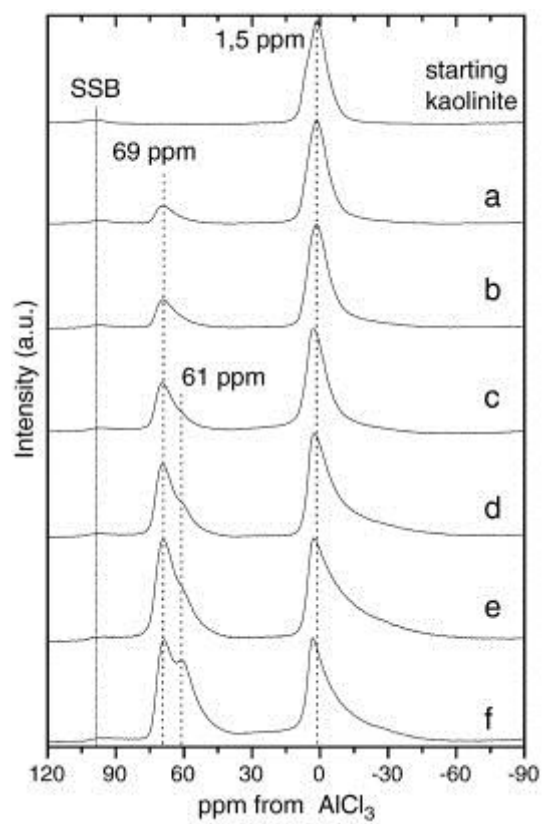


Figure 5

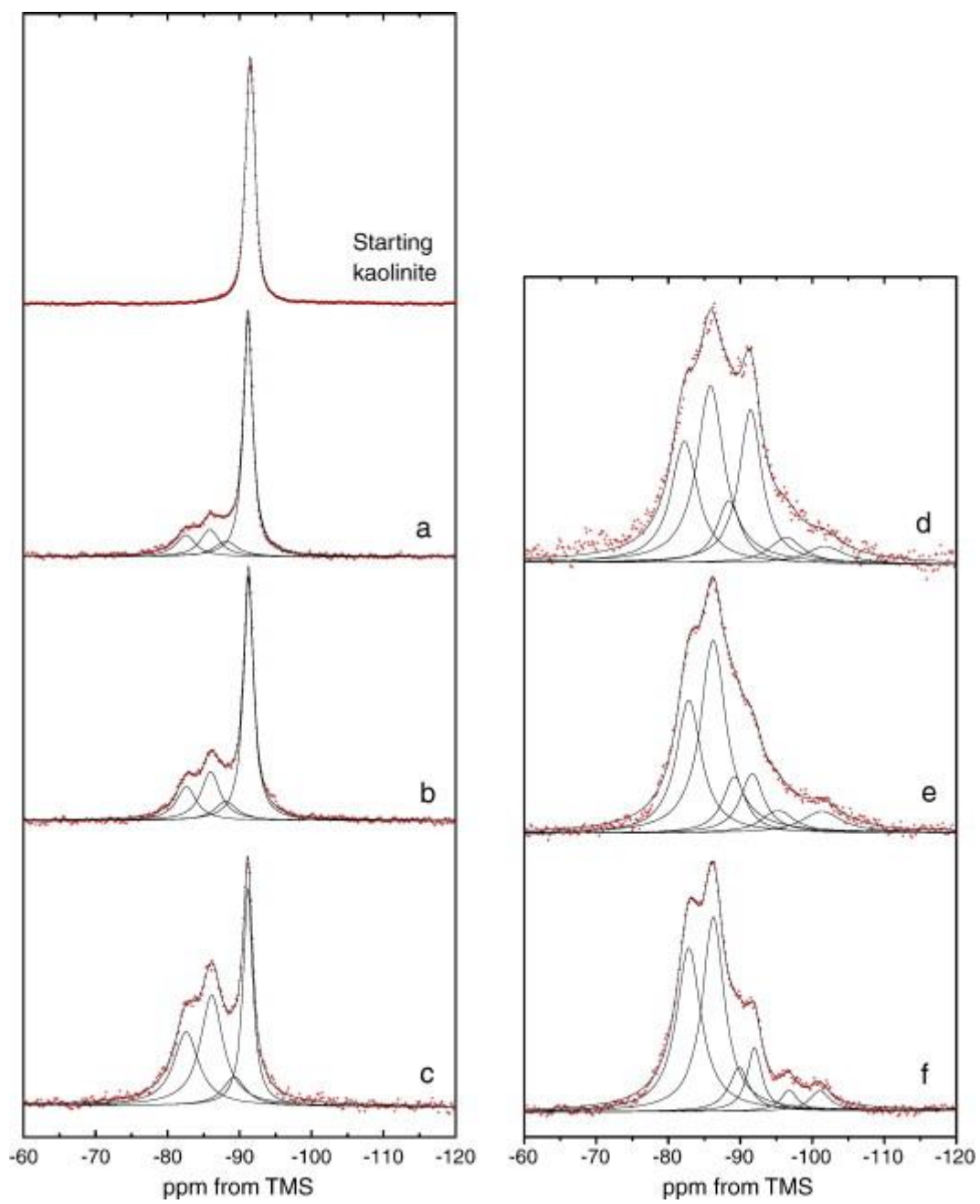




Figure 6

